

Control of the chemical structure of perhydrous coals; FTIR and Py-GC/MS investigation

Maria José Iglesias^a, José Carlos del Río^b, Fatima Laggoun-Défarge^c, Maria José Cuesta^a and Isabel Suárez-Ruiz^a

^a Instituto Nacional del Carbón (CSIC), Ap.Co., 73, 33080 Oviedo, Spain

^b Instituto de Recursos Naturales y Agrobiología (CSIC), Ap.Co., 1052, 41080 Sevilla, Spain

^c UMR 6531/FR 09 CNRS-Univ. Orléans, 45067- Orléans, Cedex 2, France

Abstract

This work analyses a set of perhydrous coals (mainly composed of huminite/vitrinite maceral group) in order to determine the inter-relations between the hydrogen content and the modifications in the coal structure at a molecular level. The study involves the direct solid state characterisation of the coal combined with the analysis of representative fragments of the coal network obtained through flash-pyrolysis. The perhydrous character of the coals is not reflected either in the aliphatic hydrogen concentration (from FTIR data) or by the presence of straight-chain aliphatic moieties in the pyrolysates. This structural study shows that perhydrous coals contain mainly aromatic structures with 1–2 rings and a very small concentration of aromatic rings of large size. In agreement with this, phenol and alkyl phenols are the most prominent degradation products whereas other aromatic compounds (mainly benzene and naphthalene derivatives) are minor and probably evaporative compounds. The major structural elements in the samples studied are simple phenols with a preponderance of substituted *para* alkyl. The results obtained show that the processes of hydrogen enrichment affect the reactions of aromatisation and condensation. During the natural evolution of the perhydrous coals the transformations of the oxygenated functionalities in the lignin precursor seem to have taken place without the parallel structural reorganisation of the lignin framework responsible for the formation of polycyclic aromatic systems. As a result, the chemical structure of perhydrous vitrinites in coals is substantially modified with respect to that described in ‘normal’ coals. The results obtained also indicate that the source of hydrogen content and the effect that it has during the subsequent evolution process of the coals, affects the chemical structure of the perhydrous vitrinite and hence its properties and behaviour.

Author Keywords: Coal; Perhydrous vitrinites; Reflectance suppression; Chemical structure; Coal structure; FTIR; Py-GC/MS

1. Introduction

Huminite/vitrinite macerals (usually the main coal components) are predominantly derived from the structural part of plants and, in general, they are deficient in hydrogen (type III kerogen). However, some vitrinites, called perhydrous vitrinites, are enriched in hydrogen, so that they resemble in some ways other types of organic matter, for example type II kerogen. Perhydrous vitrinites and perhydrous coals can originate through lipid incorporation within the biopolymers derived from lignin, cellulose or tannins. This incorporation and, therefore, the formation of perhydrous vitrinites is closely related to the redox conditions of the depositional environment and the degree of bacterial activity in the sediments [1, 2, 3, 4, 5, 6,

7, 8 and 9]. In other cases, the hydrogen enrichment of vitrinites is caused by impregnation of secondary bitumen from the surrounding environment or incorporation of oil-like substances from other sediments [10, 11, 12, 13, 14, 15, 16 and 17]. The formation of perhydrous vitrinites is also associated with the nature of the botanical precursors [17, 18, 19, 20, 21, 22 and 23]. Factors which contribute to the formation of perhydrous vitrinites are, therefore, diverse but, in all cases, the final result is a material with its physico-chemical properties substantially modified as compared to 'typical' vitrinite.

Perhydrous coals present strong anomalies in their petrological and chemical parameters related to both composition and rank [16 and 23]. The variation in hydrogen content in the huminite/vitrinite macerals is thought to play an important role in controlling reflectance values [24]. Thus, perhydrous vitrinites usually have a suppressed or abnormally low reflectance. Hydrogen-enrichment of vitrinite also affects the technological properties of coals. In particular, the peculiar behaviour of perhydrous vitrinites during heating should be mentioned, because pyrolysis is usually the basic process for coal conversion [25, 26, 27 and 28]. The anomalous properties and behaviour of perhydrous vitrinites are due to modifications in their chemical structure. It is assumed that hydrogen-enrichment of vitrinites affects the aromatisation and condensation reactions that took place during coalification [8, 16, 23 and 29] and in consequence the normal increase in their reflectance. Due to the significance of vitrinite reflectance in coal characterisation, as a rank parameter or paleogeothermometer, numerous studies which have focused on the suppression of this parameter have been carried out. Petersen and Vosgerau [15] have summarised the two main mechanisms put forward to explain vitrinite reflectance suppression. One of them refers to its perhydrous character caused by the initial hydrogen-rich vitrinitic precursor, whereas the other attributes the lowering in reflectance to bitumen-adsorption. The first mechanism is related to differences in the kinetics of the reactions involved in the increase in reflectance during coalification, and the second to the reduction in the rate of cross-linking and condensation of the aromatic framework due to bitumen adsorption. However, there is little information concerning the chemical-structural modifications of vitrinite or of the whole coal, as a result of the process of hydrogen-enrichment. In order to obtain such information a detailed structural study on these materials is required, which is not easy to obtain because of their analytical inaccessibility. In this context, the combination of a spectroscopic study of the solid material with the degradation of coal macromolecules into representative fragments is widely used in coal characterisation [30, 31, 32, 33 and 34]. Thus, it is possible to obtain information at a molecular level which complements the overall structural data from the spectroscopic analysis of the material in solid-state.

This work focuses on the study of a set of perhydrous coals in order to establish the inter-relations between hydrogen content and molecular structure and explain their anomalous properties. This is accomplished by the direct solid state characterisation of the materials combined with an analysis of representative compounds from the degradation of the coal network. The study also includes an analysis of the organic soluble fraction of the perhydrous coals.

2. Selection of samples and analytical procedures

2.1. Main characteristics of the selected samples

Two groups of perhydrous coals (for which the huminite/vitrinite maceral group is the dominant component) of different age were selected. The first group was of Cretaceous age

while the second is Jurassic. All the samples originated from drifted wood and subsequently accumulated in the depositional environment. They show the typical characteristics described for vitrain lithotype.

Cretaceous coals are naturally hydrogen-enriched coals because of the nature of their botanical precursors. These samples are denoted (Table 1) as TCV (coal of Albian age from the Teruel Basin, Spain) and UCV (Utah jet, coal of Turonian age from the Wayne County Basin in Utah, USA). The TCV sample was hand-picked from the number 4 coal seam of the Escucha Formation which is located in the underground Concepción Coal Mine (Teruel, Spain). This coal, originating in a delta–estuary depositional environment [35], has its humotelinitic structure saturated with resinite and resinite-like substances resulting from resinization processes, which took place before its incorporation in the depositional environment [23]. The UCV sample was provided by Dr J. Quick from the Utah Geological Survey (Utah, USA) and studies carried out on this material have been reported by Traverse and Kolvoord [36]. Its origin is from wood (conifer wood, probably from the Taxodiaceae family) drifted by river currents and then deposited in marine sedimentary environments.

Table 1. Sample code, location and age of the perhydrous coals^a

Sample code, location and age of the perhydrous coals ^a							
Sample Code	Provenance	Age	Reflectance values		Maceral analysis		
			Ulminite Reflectance (%)	Phlobaphinite Reflectance (%)	Ulminite (% vol)	Phlobaphinite (% vol)	Resinite (% vol)
TCV ^b	Teruel, Spain	Albian (Lower Cretaceous)	0.23	0.31	94.8	1.8	3.4
UCV	Utah, USA	Turonian (Upper Cretaceous)	0.24	---	98.6	0.0	1.4
AJV ^b	Asturias, Spain	Kimmeridgian (Upper Jurassic)	0.39	0.72	85.5	14.5	0.0
PGJV	Peniche, Portugal	Kimmeridgian (Upper Jurassic)	0.35	0.51	85.9	14.1	0.0
WJVh	Whitby, England	Toarcian (Lower Jurassic)	0.40	0.49	98.7	1.3	0.0 ^c
WJVI	Whitby, England	Toarcian (Lower Jurassic)	0.22	0.29	95.7	4.3	0.0 ^c

^a Petrographic results: reflectance (%) of huminitic components and maceral analysis (% vol., mmf).
^b Data for TCV and AJV samples were taken from Suárez-Ruiz et al. [16,23].
^c Traces of resinite.

Jurassic samples are denoted (Table 1) as: AJV (Spanish jet, coal of Kimmeridgian age from Asturias, Spain), WJVh and WJVI (Whitby jet, coals of Toarcian age from Whitby Basin, Yorkshire, England) and PGJV (coal of Lower Kimmeridgian age from the Peniche area, SW of Portugal). The AJV sample was hand-picked from a fresh coal seam. This coal originated from wood and was deposited in a transitional facies of a marine–continental sedimentary environment [37]. The origin and nature of its perhydrous character has been previously described [16]. The coal is located at the top of the Pliensbachian source-rock sedimentary series [38]. Impregnation and the adsorption of oils/hydrocarbons, generated and migrated from the Pliensbachian sediments was the process responsible for the hydrogen-enrichment of this coal [16]. The WJVh and WJVI samples were provided by the ‘Richard Tayler Minerals’ Company, England (UK). These coals, derived from fossil wood found in the Whitby Lias, correspond to the Araucaria species but are of a much larger size than those of the present day. The trees were carried away by rivers during floods, some of them reaching the sea. Decomposition of the woody material continued in a marine sedimentary environment under anaerobic conditions [39]. The properties of Whitby jet have been attributed to impregnation

by hydrocarbons generated from the parent rock [11, 12 and 17]. The last selected perhydrous sample, PGJV coal (Table 1) was provided by Dr D. Flores (University of Porto, Portugal) and Dr J. G. Prado (INCAR-CSIC, Spain). This perhydrous coal is also a jet but few data are available. It appears in an area in which the occurrence of lignite levels is common [40 and 41]. The depositional environment for this coal was probably a lagoon, shore-lake or shore swamp-like setting as demonstrated from faunal data [40]. It should be pointed out that the nature of the perhydrous character of the Whitby and Peniche coals has not been as clearly established as in the case of the AJV sample. According to the scarce data available in the literature, all of these coals are closely related to sediments or sedimentary series containing oil-shales or petroleum source-rocks. Thus, hydrocarbons, bitumens or oil-like substances could have migrated into the sedimentary horizons in which these coals are located.

2.2. Analytical procedures

An optical microscopy study was carried out with a MPV Combi Leitz microscope in reflected white light using oil immersion lenses (32 \times , 50 \times). The reflectance determinations and maceral analysis were performed following the ISO 7404/5 (1984) and ISO 7404/3 (1984) standard procedures, respectively. Observations in fluorescence were carried out with a MPVII Leitz apparatus, using water and oil immersion lenses (same magnifications) and blue-violet light excitation.

Proximate analyses were carried out following International Standard Procedures (ISO-589 1981; ISO-562 1981 and ISO 1171 1981). Ultimate analyses were performed in a LECO CHN 600 and LECO SC 132 apparatus (the oxygen content was calculated by difference) and data from Rock-Eval pyrolysis were obtained in accordance with Espitalié [42 and 43].

For the spectroscopic study (FTIR analysis) samples were prepared using the standard KBr pellet procedure for this type of material (coal:KBr mixture at a 1:100 ratio). For the semi-quantitative analysis the spectra were normalised to 1mg (daf) cm⁻² and the data given in the text are the average values of several determinations using different KBr pellets. Thus, any differences in grinding or weight between pellets are minimised. All of the absorbance spectra were recorded on a Perkin-Elmer 1750 and analysed following procedures described by Iglesias et al. [29].

A soluble fraction from each coal was obtained using chloroform as a solvent, as described in Jiménez et al. [25] and the volatile fraction was analysed by means of GC/MS. The chromatographic study was carried out on a Hewlett-Packard HP 6890 gas chromatograph equipped with flame ionisation detection (FID) and the identification of the compounds was performed by means of GC/MS using a Finningan GCQ gas chromatograph equipped with mass detection. The experimental conditions used were the same as those previously reported by Jiménez et al. [44].

The molecular characterisation of the perhydrous vitrinites was carried out through Curie-point flash-pyrolysis-gas chromatography-mass spectrometry. The pyrolysis was performed at 610°C using a Varian Saturn 2000 GC-MS equipment, with a 30 m \times 0.25 mm DB-5 column (film thickness 0.25 μ m), coupled to a Curie-point pyrolyser (Horizon Instruments Ltd.). Approximately 100 μ g of finely ground sample was deposited on a ferromagnetic wire, then inserted into a glass liner and immediately placed in the pyrolyser. The chromatograph was programmed from 40°C (1 min) to 300°C at a rate of 6°C min⁻¹. The final temperature was held for 20 min. The injector, equipped with a liquid carbon dioxide cryogenic unit, was

programmed from -30°C (1 min) to 300°C at $200^{\circ}\text{C min}^{-1}$, while the GC–MS interface was kept at 300°C . The compounds were identified by comparing the mass spectra with those of the Wiley and Nist computer libraries and by mass fragmentography.

3. Results and discussion

3.1. Petrological characteristics of the perhydrous coals

Megascopically, the coals selected in this study are black, bright, with a glassy lustre, hard and compact showing conchoidal fracture. They are light-weight, easy to polish and with the exception of the TCV sample, they have no cracks.

The results from the petrographic analysis are shown in Table 1 and in Plate 1, Plate 2. In general, all the coals are characterised by a very low content of mineral matter. The Cretaceous samples, TCV and UCV, are composed of ulminite (humotelinite) as the dominant maceral with minor amounts of resinite (Table 1) filling the cell cavities, resinite being more abundant in TCV coal (Plate 1a–e). Phlobaphinite was identified only in TCV [23] as a very scarce and non-fluorescent component of 0.31% reflectance, in cell cavities of ulminite. In both coals, ulminite has a very low reflectance value (0.23–0.24% respectively, Table 1) with a fluorescence that varies in intensity and colour from orange–brown in the TCV sample to dark red–brown in the UCV coal. Moreover, in the latter sample, ulminite shows different degrees of gelification but a very well preserved structure (Plate 1c, e). In both coals, two types of resinite were detected in the cell cavities of botanical tissues mainly on the basis of their fluorescence colour which varies from a very intense yellow (most common) to an orange colour of low intensity. Exsudatinite [23] was also detected in fluorescence mode as a secondary and very scarce component of homogeneous orange colour.

The AJV and PGJV coals show similar petrographic composition (Table 1). Both are made up of the huminite/vitrinite maceral group with ulminite (humotelinite) and phlobaphinite (humocollinite) macerals occurring in different proportions (Plate 2a–c). Resinite was not detected in these coals. Ulminite has relatively well-preserved cell walls and cavities. These cellular cavities are filled with phlobaphinite. This component also occurs as segregations mixed with ulminite. The main differences between the two coals are that ulminite in the AJV sample shows an intense fluorescence [16] of orange colour whereas the ulminite in PGJV displays very weak fluorescence (red–brown colour of very low intensity). Phlobaphinite never shows fluorescence properties (Plate 2b). This maceral is of variable size, greater in the case of the PGJV sample and frequently presents an irregular porosity. The reflectance values of ulminite and phlobaphinite in the PGJV coal (0.35 and 0.51% respectively) are clearly lower (Table 1) than those shown by the same components in the AJV sample (ulminite reflectance: 0.39% and phlobaphinite reflectance: 0.72%).

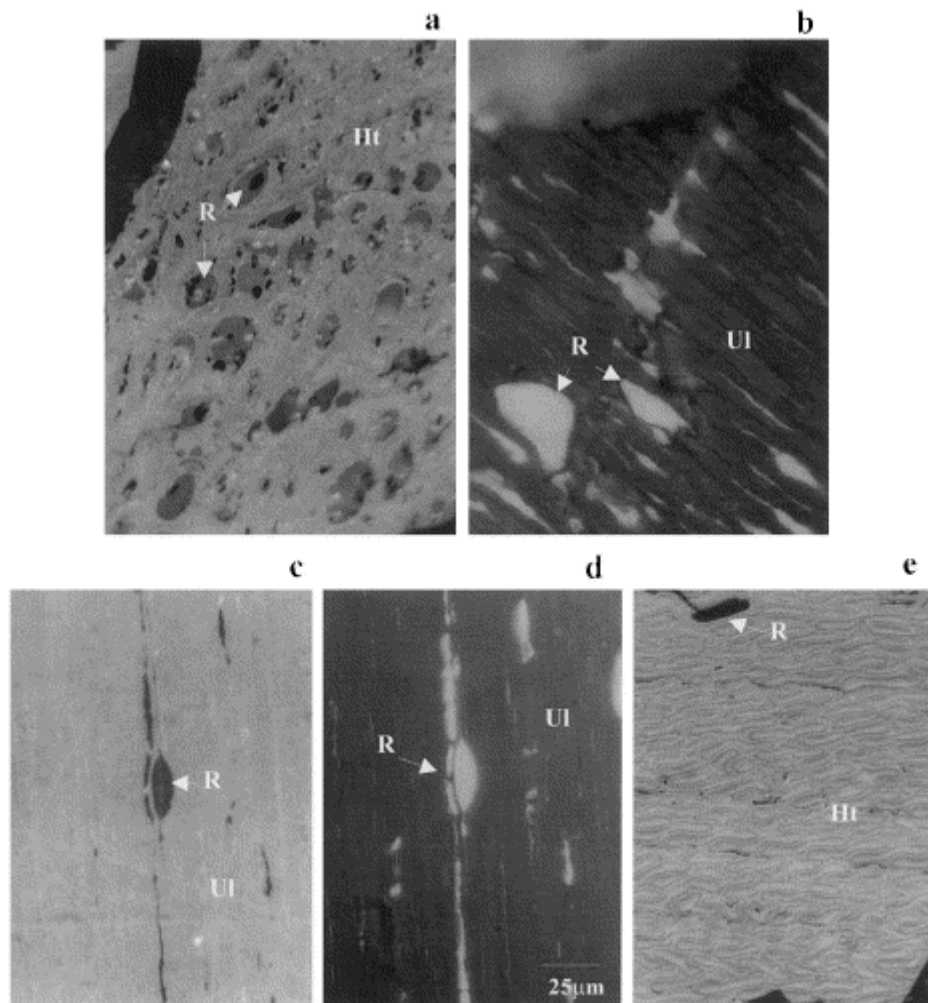


Plate 1. Photomicrographs of the perhydrous coals (reflected white light and blue-violet excitation modes, oil immersion). (a) TCV coal, white light, humotelinite (Ht) (ulminite) and resinite (R) in cell cavities. (b) TCV coal, fluorescence mode, ulminite (Ul) with fluorescence of low intensity and resinite (R, yellow colour) in compressed cell cavities. (c) UCV coal, white light, ulminite (Ul) and resinite (R). (d) UCV coal, same field in fluorescence mode. (e) UCV coal, white light, humotelinite (Ht): well preserved botanical tissue and dark resinite (R) in some cell cavities.

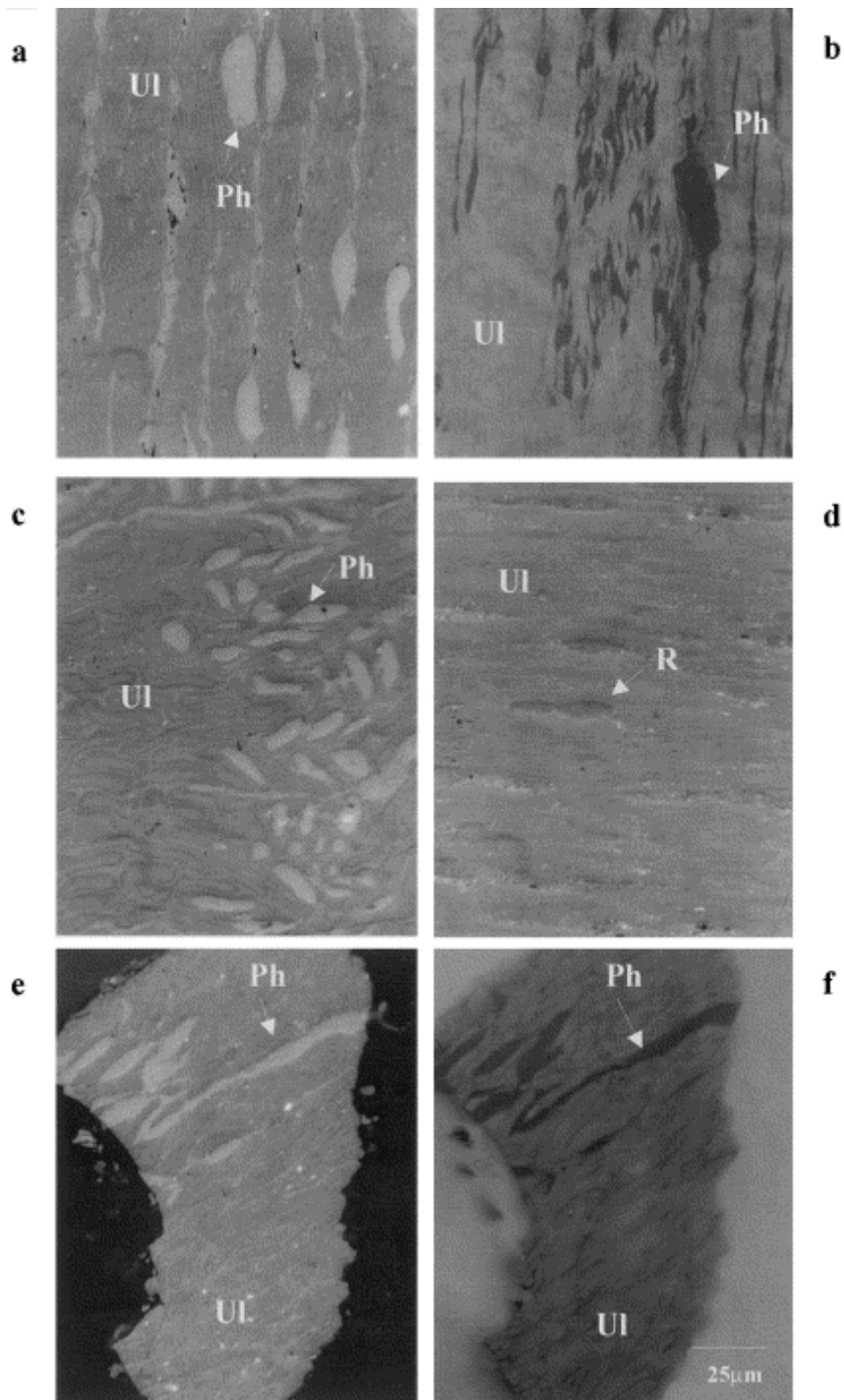


Plate 2. Photomicrographs of the perhydrous coals reflected white light and blue-violet excitation modes, oil immersion. (a) AJV coal, white light, ulminite (Ul, humotelinite) and phlobaphinite (Ph, humocollinite). (b) AJV coal, fluorescence mode, ulminite (Ul) with orange colour and phlobaphinite (Ph) without fluorescence. (c) PGJV coal, white light, ulminite (Ul): preserved cell structure and phlobaphinite (Ph). (d) WJVh coal, white light, ulminite (Ul) and scarce resinite (R). (e) WJVI coal, white light, ulminite (Ul) and phlobaphinite (Ph). (f) WJVI coal, fluorescence mode, ulminite (Ul) with intense colour showing the botanical structure and non-fluorescent phlobaphinite (Ph).

WJVI and WJVh coals are composed of ulminite with different degrees of gelification (Plate 2d, e). Phlobaphinite is a minor component that fills cell cavities and shows the typical features described above (Plate 2e and f). This component is more abundant in the WJVI

sample (Table 1), but its reflectance is lower than in the case of the WJVh coal (Table 1). Traces of resinite inside cell cavities were also detected especially in WJVh coal (Plate 2d). Resinite fluoresces with low intensity of dark brown colour. In the WJVI coal resinite shows an intense yellow colour. Ulminite in WJVI coal with a reflectance value of 0.22% is less evolved (Table 1), but its appearance is occasionally more homogeneous than in the case of WJVh and it exhibits a highly intense fluorescence of an orange–yellow colour. On the other hand, the highly reflecting ulminite (0.40% reflectance, Table 1) in WJVh is not fluorescent or it has a very low intensity dark brown colour in which the fluorescence of resinite can be observed. This coal reflects a higher degree of evolution but has a heterogeneous appearance and a porous texture in which botanical structures can be observed.

3.2. Global geochemical characteristics

Results from proximate and ultimate analyses for the perhydrous coals are given in Table 2. The elemental composition of the WJVI sample is very close to that reported for the Whitby jet [45] and it shows higher values of hydrogen and volatile matter content than the WJVh coal. Assuming that the hydrogen content (or H/C atomic ratio) affects the vitrinite reflectance values greatly, the lower vitrinite reflectance obtained for WJVh with respect to WJVI (Table 1) could be due, at least in part, to differences in hydrogen content.

Table 2. Results of the proximate and ultimate analysis, atomic ratios and parameters from Rock–Eval pyrolysis for the perhydrous coals

Sample	Proximate analysis			Ultimate analysis					Atomic ratios		Rock-Eval		
	Moisture (%)	Ash (% dry)	V.M. (% daf)	C (% daf)	H (% daf)	O _{air} (% daf)	N (% daf)	S _{org} (% daf)	H/C	O/C	T _{max} (°C)	S ₁ (mg HC/g sample)	S ₂ (mg HC/g sample)
TCV	12.9	3.1	62.4	79.7	6.2	11.3	0.5	2.3	0.93	0.11	397	0.9	291
UCV	5.1	1.8	60.2	77.3	5.9	13.7	0.7	2.3	0.92	0.13	404	2.6	305
AJV	2.9	1.1	54.9	84.8	5.9	7.5	0.9	1.0	0.83	0.07	417	2.9	365
PGJV	2.6	1.4	57.1	80.5	5.7	11.0	0.9	1.9	0.84	0.10	415	10.2	303
WJVh	7.3	2.4	52.1	82.4	5.7	10.1	1.2	0.6	0.83	0.09	425	3.5	250
WJVI	1.7	2.5	72.1	82.6	7.4	6.6	1.2	2.2	1.07	0.06	425	57.9	473

All samples are characterised by an almost pure organic composition (ash content $\leq 3.1\%$, Table 2). The moisture content of the AJV, PGJV and WJVI samples is very low (1.7–2.0%, Table 2). Given the humic origin and petrographic composition of the coals, their position on the van Krevelen diagram [46] clearly reflects their perhydrous character (Fig. 1a). WJVI shows the strongest hydrogenated character (highest H/C atomic ratio) and WJVh seems to be the less affected by hydrogen-enrichment. The relative positions of the AJV and PGJV coals seem to be consistent with the values of phlobaphinite reflectance (Table 1). The close position of the WJVh, PGJV and TCV samples (Fig. 1a) suggests a similar degree of evolution for these coals despite the different values of vitrinite reflectance (Table 1). For TCV, such a position seems, therefore, to be closely related to its real degree of evolution (beginning of the bituminisation interval) [23 and 25].

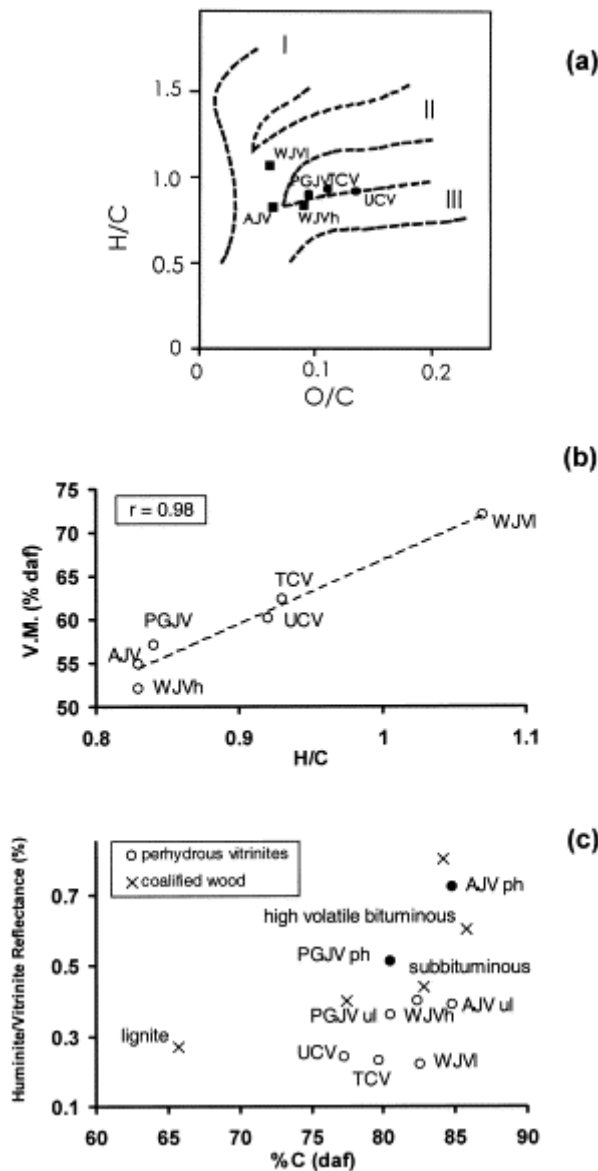


Fig. 1. (a) Location of the perhydrous coals in the van Krevelen diagram [46]. (b) Correlation between the volatile matter content and the H/C atomic ratio. (c) Vitrinite reflectance (%) versus carbon content (dry ash free basis) for the perhydrous coals and comparison with data reported in the literature [30, 31, 32 and 33].

Perhydrous coals are also characterised by a high volatile matter (52–73% daf, Table 2). The H/C atomic ratio and volatile matter content are closely interrelated (Fig. 1b) and indicate a low degree of aromatisation/condensation. The volatile matter content of WJVh is the lowest of all the selected samples reflecting again its less pronounced perhydrous character.

The values of the carbon content (77–85% daf, Table 2) are high in comparison with other parameters (volatile matter content and vitrinite reflectance). The discrepancies between carbon content and vitrinite reflectance for perhydrous coals [16, 23, 25 and 36] are in this case shown in Fig. 1c. Here, the vitrinite reflectance values of the coals are plotted versus carbon content and compared with the values shown in the literature for different coalified woods [30, 31, 32 and 33]. Samples of coalified wood were chosen for comparison because they have a similar origin to the actual selected perhydrous coals (drifted wood) and also because all the samples are of the Mesozoic age. TCV, UCV and WJVI coals show very low values of vitrinite reflectance, typical of the lignite coal rank, whereas their carbon content is

closer to samples of the subbituminous coal rank. For the AJV and PGJV samples the carbon content is more consistent with the values of phlobaphinite reflectance than with the extremely low values of the ulminite. Finally, the discrepancies between carbon content and vitrinite reflectance are less pronounced in WJVh than in the other samples. Given that this sample seems to be less affected by the process of hydrogen-enrichment, its value of vitrinite reflectance might be expected to be less suppressed.

The perhydrous coals show very low values of T_{\max} (Table 2), the Cretaceous samples (TCV and UCV) having the lowest values. In the correlation between T_{\max} and vitrinite reflectance [47] samples are located in the less evolved coals region (Fig. 2). For the TCV, UCV, AJV, PGJV and WJVh samples the correlation between these two parameters is good ($r=0.92$) but such a correlation is not found when WJVI sample is included. This is because the value of T_{\max} for WJVI is significantly higher than that found for TCV and UCV (Table 2).

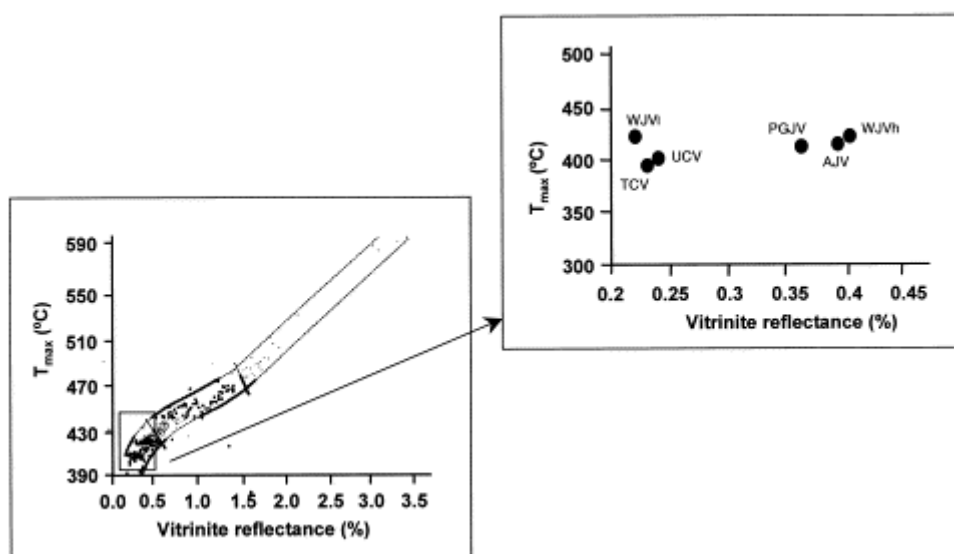


Fig. 2. Evolution trend of vitrinite reflectance (%) versus T_{\max} (°C) as reported by Teichmüller et al. [47]. Location of the perhydrous coals in the correlation band. (For Jurassic coals, values of ulminite reflectance from Table 1 were considered).

The S1 parameter normally indicates the amount of free hydrocarbons that there are in a specific sample [42 and 43]. In the case of perhydrous coals, this parameter might also indicate the amount of bitumen or oil-like substances in the microporosity of the coal matrix. This is certainly the case of PGJV and WJVI with high values of S1 (10.2–57.9 mg HC/ g sample, respectively) but it is not the case for the other two samples AJV and WJVh (2.9–3.5 mg HC/g sample). For these samples (AJV and WJVh) S1 values are similar to those of the UCV coal (Table 2). It is well known that some occluded aromatic hydrocarbons can only be released from the coal matrix after treatment at 350–400°C due to their restricted mobility [48]. The existence of strong interactions between the assimilated substances and the vitrinite matrix in AJV and WJVh is supported by the strong swelling of these samples (free swelling index of $5\frac{1}{4}$ and 5, respectively [16 and 28]). Given the very low rank of these samples these F.S.I. values (Free Swelling Index) do not correspond to the development of plasticity, but are more likely due to the release of compounds from the huminite/vitrinite structure. The lower S1 values for AJV and WJVh (Table 2) compared to the other coal samples suggest, therefore, chemical–structural differences in the substances occluded in the vitrinite network.

For the perhydrous coals the S2 values (Table 2) are high in all cases (≥ 250 mg HC/g sample). For the WJV1 and WJVh coals, S2 presents the highest and lowest value respectively (Table 2), which corresponds to the different extent of the perhydrous character of these vitrinites. Furthermore, as was suggested above, in WJVh S2 might also be increased by the contribution of the hydrogenated compounds contained in the samples. Such an effect is also very likely to occur in the AJV coal [16]. A comparison of the S2 values with those of the H/C atomic ratio (Table 2) for AJV, PGJV, TCV and UCV does not show a clear correlation between these two parameters. This suggests that the S2 peak from Rock-Eval could be affected not only by the high hydrogen content but also by the source of this hydrogen content.

3.3. Spectroscopic study (FTIR)

Fig. 3 shows the FTIR spectra of the perhydrous samples. The assignments of the different regions of the spectra are depicted at the top of the figure. The results from the semi-quantitative analysis are shown in Table 3. The spectra and data for the TCV and AJV samples previously reported [29] are also presented here for comparative purposes. It can be seen that the spectra from the UCV and WJVh/WJV1 samples closely resemble those reported for the Utah and Whitby jets, respectively [12 and 36].

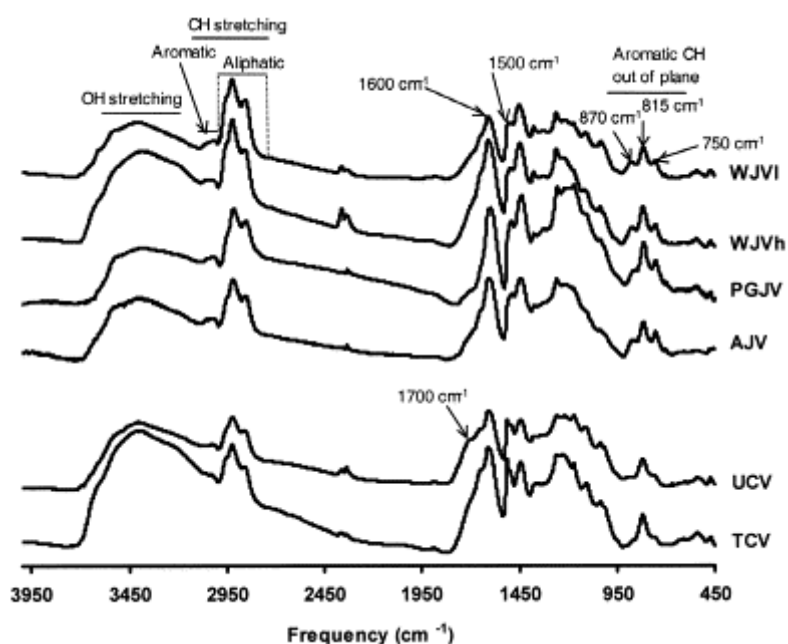


Fig. 3. FTIR spectra of the perhydrous coals showing the assignment of the different spectral regions.

A quick look at the spectra (Fig. 3) is enough to distinguish the two groups of samples, Cretaceous (TCV and UCV) and Jurassic (AJV, PGJV, WJVh and WJV1). The main difference found is the intensity of the aromatic modes at 1500 and 815 cm^{-1} . Cretaceous coals show a higher intensity for these two bands than in the case of the Jurassic samples. The preponderance of the band at 815 cm^{-1} and the presence in coals of a clear absorption at 1500 cm^{-1} have been attributed to a lower degree of condensation/substitution of aromatic units [49, 50 and 51]. At the same time, the 1500 cm^{-1} mode is also affected by the nature and position of the substituents on the benzene ring [52]. This band arises from a mode in which the dipole-moment change is produced by the relative movements of the substituents on opposite sites of the ring, both moving in the same direction. This implies a preponderance of

para-substitution which explains the relation between the intensity of this band (1500 cm^{-1}) and that at 815 cm^{-1} (two and/or three adjacent aromatic CH groups). Furthermore, the reasonable correlation between the relative intensity of the 815 cm^{-1} mode (%815 in Table 3) and the O/C atomic ratio (Table 2) given in Fig. 4a confirms the reported [53] relation between these spectral features (band at 1500 cm^{-1} and the relative intensity of the 815 cm^{-1} band) and the presence of *para*-alkyl substituted phenols as the major structural units in the perhydrous coals studied.

Table 3. FTIR data (arbitrary units) for the perhydrous coals^f

Sample	Har ^a	Hal ^b	Har/Hal	%870 ^c	%815 ^d	%750 ^e
TCV	0.13	6.45	0.02	~ 10	~ 70	~ 20
UCV	0.28	8.24	0.03	~ 8	~ 74	~ 18
AJV	0.65	8.83	0.07	23	46	31
PGJV	0.51	8.15	0.06	14	55	31
WJVh	0.46	12.41	0.04	22	53	25
WJVI	0.28	10.94	0.02	21	52	27

^a Har: integrated area between 3100 and 3000 cm^{-1} (aromatic CH stretching vibrations).

^b Hal: integrated area between 3000 and 2700 cm^{-1} (aliphatic CH stretching vibrations).

^c %870 = $\text{Abs}870/(\text{Abs}870 + \text{Abs}815 + \text{Abs}750)$.

^d %815 = $\text{Abs}815/(\text{Abs}870 + \text{Abs}815 + \text{Abs}750)$.

^e %750 = $\text{Abs}750/(\text{Abs}870 + \text{Abs}815 + \text{Abs}750)$.

^f Data for TCV and AJV samples were taken from Iglesias et al. [29]

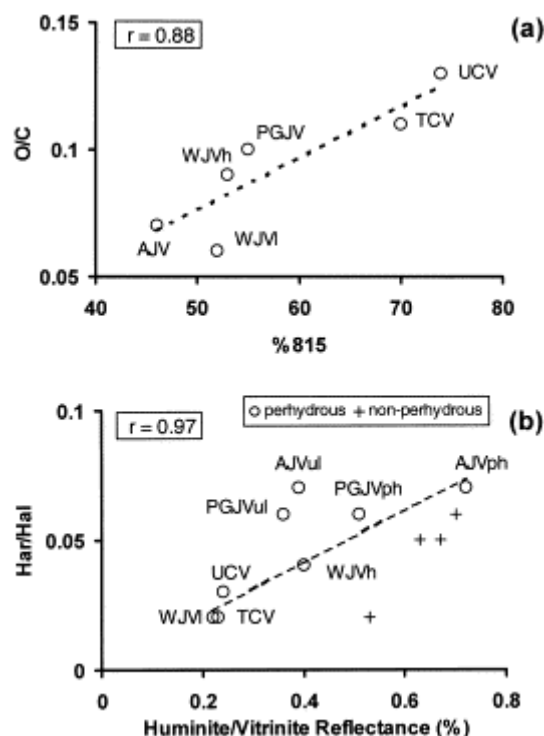


Fig. 4. (a) Relationship between the relative intensity of the infrared mode at 815 cm^{-1} (%815) and the O/C atomic ratio. (b) Plot of the Har/Hal ratio versus vitrinite reflectance of perhydrous coals and comparison with data reported in the literature [29] for non-perhydrous samples.

The TCV, UCV and WJV1 samples show a lower aromaticity (see Har and Har/Hal values in Table 3) than the other samples (AJV, PGJV and WJVh). For the WJV1 coal, however, the distribution of the aromatic hydrogen is much closer to that found in AJV, PGJV and WJVh than in the TCV and UCV samples. The low aromaticity of WJV1 should be interpreted as a result of the higher aliphatic content in this sample than in the others. Aromaticity apparently agrees with the vitrinite reflectance values (Table 1). However, a comparison of the Har/Hal values for the perhydrous samples with the data from non-perhydrous coals [29], depicted in Fig. 4b, shows in all cases higher values of Har/Hal than those expected for the values of vitrinite reflectance. For the AJV and PGJV samples aromaticity seems to be more consistent with the reflectance of phlobaphinite than with that of the ulminite (main component, Table 1) as is inferred through the linear correlation between Har/Hal and vitrinite reflectance ($r=0.97$ with phlobaphinite reflectance; $r=0.83$ with ulminite reflectance, Fig. 4b). Furthermore, in the samples studied here the distribution of aromatic hydrogen (Table 3) differs from that usually found in non-perhydrous coals [29 and 54]. The aromatic structures in non-perhydrous coals are mainly pentasubstituted (870 cm^{-1} mode) whereas in the perhydrous coal studied here the band at 815 cm^{-1} is the most prominent of the aromatic C–H out-of-plane bending modes. This indicates a preponderance of aromatic systems containing 1–2 rings with a very small contribution of large size aromatic rings [51].

The extent of the perhydrous character of the samples studied (Table 2, Fig. 1a) is not reflected in the intensity of the aliphatic C–H stretching modes (Hal in Table 3). Thus, the highest value for this parameter (Hal) was found for the samples with the more and less pronounced perhydrous character, WJV1 and WJVh, respectively. This implies the existence of structural differences in the aliphatic moieties of the coals which could affect the extinction coefficients of the aliphatic stretching modes. The concentration of aliphatic hydrogen in the samples cannot, therefore, be estimated by merely measuring the intensity of the modes.

3.4. Composition of the volatile fraction (GC/MS analysis) from the soluble organic matter of perhydrous coals

Fig. 5 shows the chromatograms of the soluble organic fraction of the perhydrous samples and a list of the major compounds identified is given in Table 4. Qualitatively, the TCV and UCV extracts are made up of the degradation products of terpene-type resinite as might be expected considering that resinite and resinite-like substances were significant components of these samples (Table 1). Cadalene (peak L), a typical biomarker of resins is the major compound in both extracts. 1,6-Dimethylnaphthalene (peak F2) another typical biomarker of resins is, apart from 2,6- and/or 2,7-dimethylnaphthalene (peak F1), the most abundant isomer of C2-naphthalenes. The soluble organic fractions also contain a significant amount of C₁₅H₂₄ alkylbenzene (peak H), identified as 1,3-dimethyl-1,2-heptylbenzene (Fig. 5 and Table 4). The largest m/z at 119 in the mass spectrum of this compound is consistent with an isoprenoid structure following by dehydrogenation [55]. Tetrahydronaphthalenes (peaks E and I) with a molecular weight of 174 and 188, respectively show a large $M^+ - \text{CH}_3$ fragment ion which suggests the presence of a *gem*-dimethyl group on the saturated ring. This kind of compound is believed to derive from bicyclic-sesquiterpanes [55]. Tetrahydroretene and retene (peaks S and V) are considered the result of the diagenetic aromatisation of abietic acid, a common constituent of conifers [56]. Finally, another compound probably related to terpenoid precursors is nonil-phenol (peak N). It is assumed that the cracking of triterpenoid compounds into sesquiterpenoids could produce long-chain phenols [57].

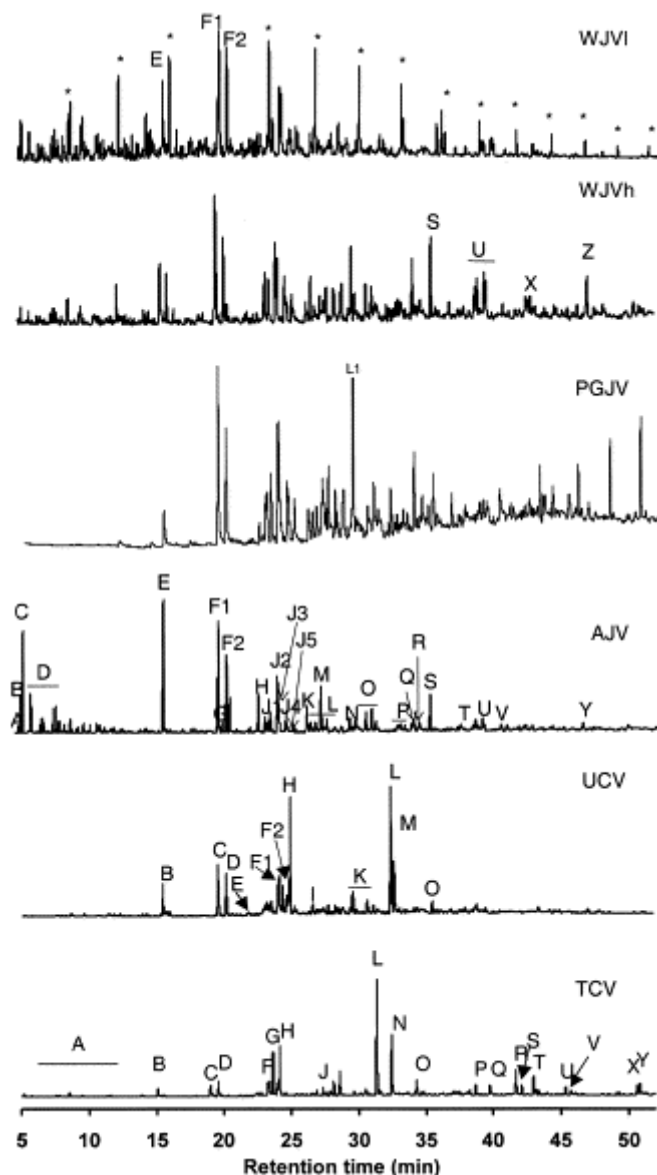


Fig. 5. Gas chromatograms of the soluble organic fraction of perhydrous coals (see Table 4 for peak identification, * *n*-alkanes).

The semi-quantitative data obtained from the chromatograms of TCV and UCV extracts are shown in Fig. 6a. For this figure, the peak areas of the major compounds in the chromatograms were measured and the relative proportions of the different components were also normalised to the largest peak in the chromatogram (cadalene, peak L in Fig. 5). In general terms, a higher proportion of compounds eluting before (after) cadalene in UCV (TCV) than in the TCV (UCV) soluble organic fraction can be observed. A higher preponderance of β -isomers of alkyl naphthalenes in the UCV compared to the TCV extract (see the relative contribution of 2- and 1-methyl naphthalene in Fig. 6a) suggests a higher degree of evolution in UCV than in the TCV coal. However, possible differences in rank may not be the only explanation for the distribution of alkyl naphthalene derivatives.

Table 4. Major compounds identified by GC/MS in the soluble organic fractions of (a) Cretaceous and (b) Jurassic perhydrous coals (for peak code see Fig. 5)

Peak code	Compound (a)	Peak code	Compound (b)
A	C2- to C4-alkylbenzenes	A	Ethylbenzene
B	Naphthalene	B	<i>m-p</i> -Xylene
C	2-methylnaphthalene	C	<i>o</i> -Xylene
D	1-methylnaphthalene	D	C3- and C4-benzenes
E	Alkyl-tetrahydronaphthalene	E	Naphthalene
F	C2-naphthalenes	F1	2-methylnaphthalene
F1	2,6- and/or	F2	1-methylnaphthalene
	2,7-dimethylnaphthalene		
F2	1,6-dimethylnaphthalene	G	Dimethyltetrahydronaphthalene
G	Alkylcyclohexane	H	Biphenyl
H	Alkylbenzene	I	Ethyl-naphthalenes
I	Alkyl-tetrahydronaphthalene	J1	2,6- and/or 2,7-dimethylnaphthalene
J	C3-naphthalene	J2	1,3- and/or 1,7-dimethylnaphthalene
K	C4-naphthalene	J3	1,6-dimethylnaphthalene
L	Cadalene	J4	2,3 and/or 1,4-dimethylnaphthalene
M	C5-naphthalene	J5	1,5-dimethylnaphthalene
N	Nonilphenol	J6	1,2-dimethylnaphthalene
O	Phenanthrene	K	Methylbiphenyls
P	Hydroxicadalene	L	C3-naphthalenes
Q	Elemental sulphur	M	Dibenzofuran
R	Fluoranthene	N	Fluorene
S	Tetrahydroretene	O	Methyl-dibenzofurans
T	Pyrene	P	Methylfluorenes
U	Benzofluorene	Q	C2-biphenyls
V	Retene	R	Dibenzothiophene
X	Benzoanthracene	S	Phenanthrene
Y	Chrysene/Triphenylene	T	C3-dibenzofurans
		U	Methylphenanthrenes
		V	Dihdropyrene
		X	Dimethylphenanthrenes
		Y	Benzofluorene
		Z	Retene

It is also possible that these compounds do not occur in proportions determined by thermodynamic control but by the isomers derived from the degradation of terpenoid precursors [58]. The latter explanation seems to be the most feasible. The increase in the relative proportion of 2-methylnaphthalene attributed to the thermal rearrangement of 1-methylnaphthalene occurs beyond 0.95% of vitrinite reflectance when the methyl groups show an enhanced mobility [59]. Such a degree of evolution disagrees with the optical properties (both in white light and in fluorescence modes) found for resinities in these samples. Thus, differences in the composition of the soluble organic fractions from TCV and UCV seem to be related to differences in the botanical precursors of these coals as well as in the physico-chemical conditions that existed in the corresponding depositional environments.

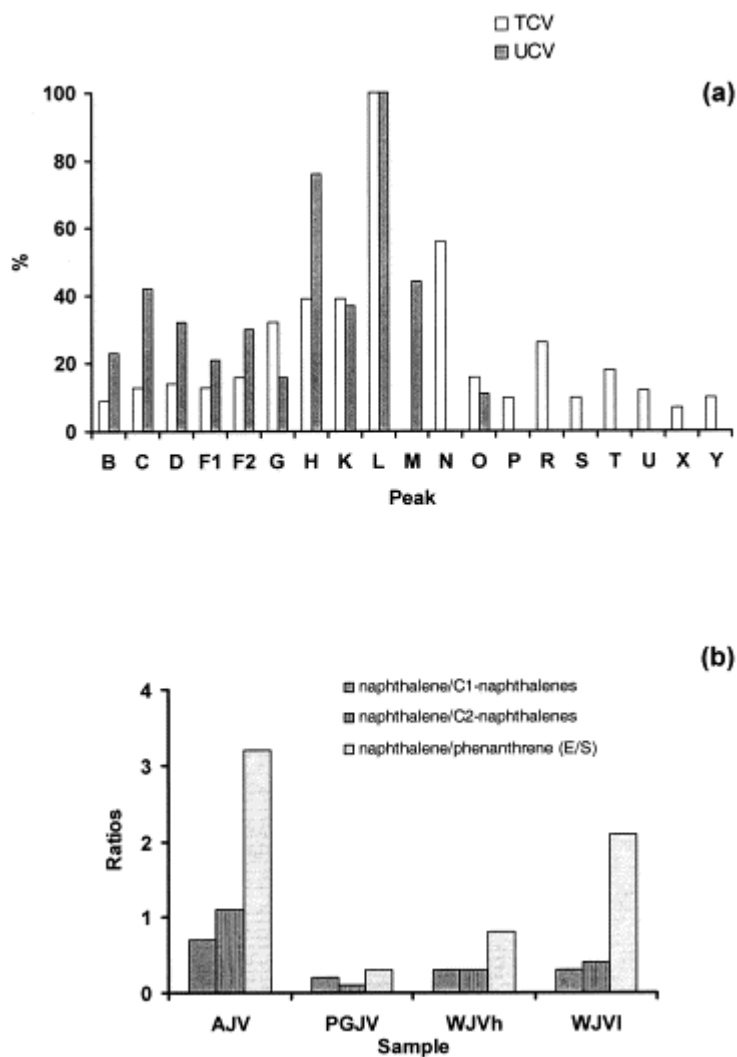


Fig. 6. Semi-quantitative GC data of the soluble organic fraction derived from the perhydrous coals. (a) Cretaceous coals (TCV and UCV), peaks areas were calculated to the largest peak in the chromatogram (cadalene, peak L). (b) Jurassic coals (AJV, PGJV, WJVh, WJVI).

The composition of the extracts derived from Jurassic coals: AJV, PGJV, WJVh and WJVI (Fig. 5) shows that they differ strongly in aliphatic content (*n*-alkanes). *n*-Alkanes were identified in the WJVI and WJVh samples whereas the nature of the AJV and PGJV extracts is entirely aromatic. *n*-Alkanes are very important constituents of the WJVI soluble organic fraction with a preponderance of these in the C₁₃–C₁₇ range and a relative odd/even equilibrium typical of marine sedimentary environments as can be observed through the fragmentograms *m/z* 57 and *m/z* 99 given in Fig. 7a. The amount of *n*-alkanes in the WJVh extract is lower than in the WJVI sample and the relative proportion in the C₁₆–C₂₃ range undergoes a drastic decrease in the WJVh extract (Fig. 7b). *n*-Alkanes cannot be directly derived from lignin, the main biopolymer precursor of huminite/vitrinite (the major component of these coals). Consequently the presence of these compounds in WJVI and to a lesser extent in the WJVh extracts, indicates the incorporation of other components into the coal matrix. This finding agrees with the introduction of lipoidal or bituminous substances within the huminite/vitrinite structure during diagenesis, a hypothesis put forward to explain the properties of Whitby jet [11, 12 and 17]. Furthermore, the higher contribution of these compounds in the WJVI coal confirms the view that there was a larger incorporation of

aliphatic material into this sample that could explain at least in part the low aromaticity (Table 3) and the high H/C atomic ratio and S1 value (Table 2).

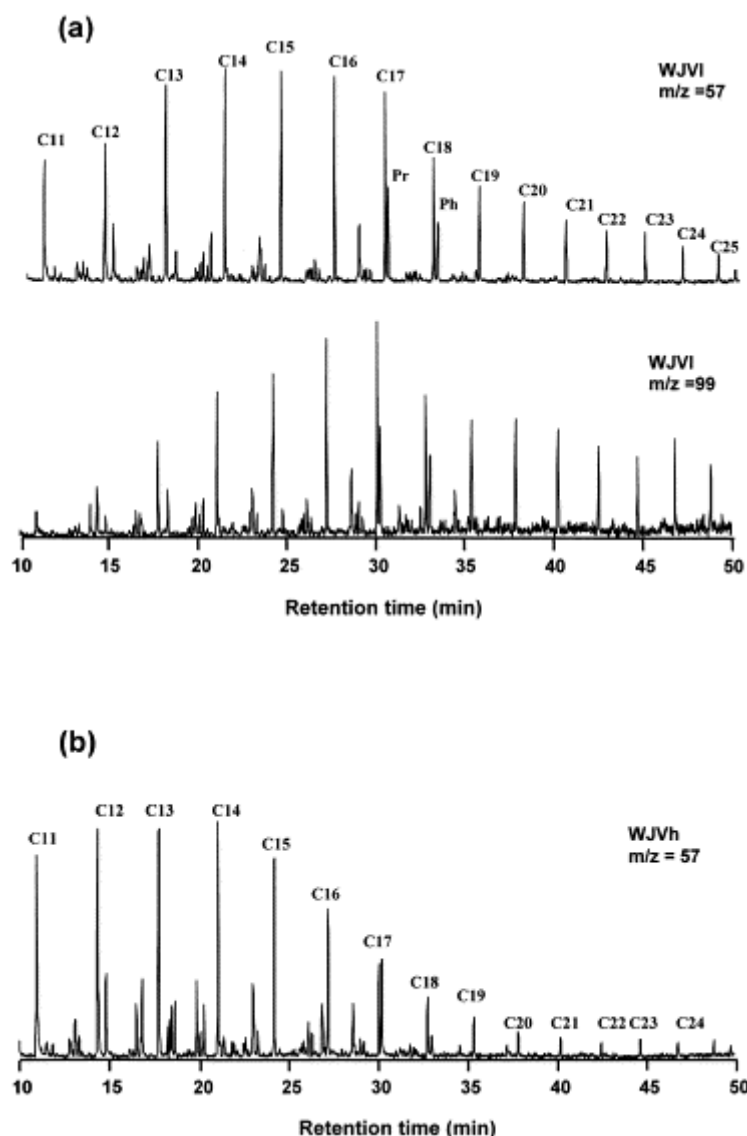


Fig. 7. (a) m/z 57 and m/z 99 mass fragmentograms showing the alkane distribution for the WJVl extract. (b) m/z 57 mass fragmentogram for the WJVh extract.

With regard to aromatic compounds, the AJV, PGJV, WJVh and WJVl extracts contain the same families with a preponderance of naphthalene derivatives (Fig. 5 and Table 4). Fig. 6b shows there is a preponderance of naphthalene over alkyl naphthalene derivatives in the AJV sample. In the WJVh and PGJV soluble organic fractions there is also an important contribution of C3-alkyl naphthalene derivatives (peaks L) with a preponderance of 1,2,5-trimethylnaphthalene (peak L1). Fig. 6b also shows the naphthalene (peak E) to phenanthrene (peak S) ratio. In the AJV and WJVl extracts naphthalene predominates over phenanthrene and the highest value of this ratio is found for the AJV extract. In the WJVh sample, however, the amounts of naphthalene and phenanthrene are very close, whereas in the PGJV extract phenanthrene preponderates.

All of the samples show a clear preponderance of the most thermally stable configurations for the C1- and C2-naphthalenes [59 and 60] (Fig. 5 and Table 4). However, the distribution of C2-naphthalenes in AJV extract is different to that found in the other extracts. In this extract 1,3-/1,7-dimethylnaphthalene (peak J2) clearly dominates in the volatile fraction, whereas in the other extracts the proportion of this isomer and 1,6-dimethylnaphthalene (peak J3) is very similar (Table 5). The 2-methylnaphthalene to 1-methylnaphthalene ratio (Table 5) is similar for all the samples, and it is too high to be attributed to the rank of the coals [58]. A better explanation for such high values is that soluble fractions are mainly made up of the substances assimilated/adsorbed within the coal matrices. The differences found in the composition of the extracts derived from the Jurassic samples therefore show the different origin or nature of the substances which have been assimilated by the coal structure of these samples.

Table 5. 1,3-+1,7-dimethylnaphthalene to 1,6-dimethylnaphthalene and 2-methylnaphthalene to 1-methylnaphthalene ratios for the soluble organic fractions derived from Jurassic coals

Sample	1,3- + 1,7-DMN/1,6-DMN	2-MN/1-MN
AJV	2.1	1.7
PGJV	1.3	1.7
WJVh	1.2	1.5
WJVI	1.1	1.5

3.5. Molecular characterisation of perhydrous coals (Curie-point flash-pyrolysis–gas chromatography–mass spectrometry analyses)

Fig. 8 shows the chromatograms of the flash pyrolysates derived from perhydrous coals and Table 6 provides an identification of the peaks. Except for the WJVI sample, the nature of the pyrolysates is entirely aromatic. In the WJVI pyrolysate traces of *n*-alkanes were detected through the fragmentogram *m/z* (57+71) as can be seen in Fig. 9. This agrees with the composition of its extract described above (Fig. 5).

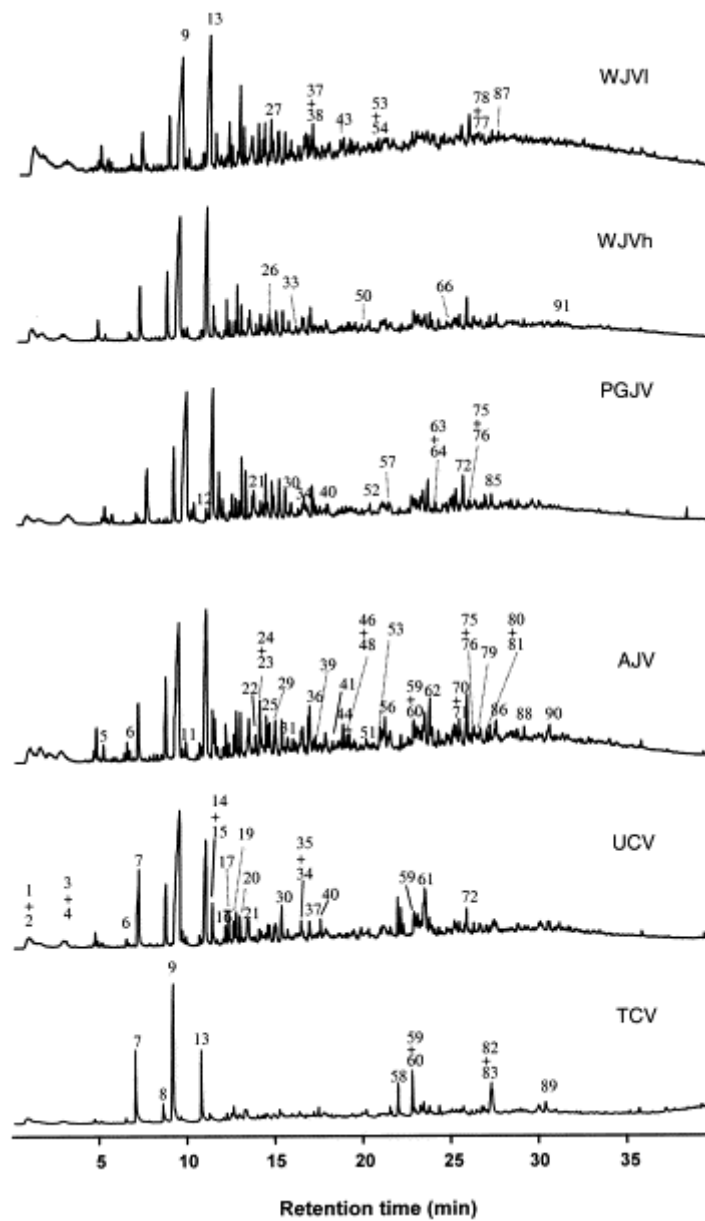


Fig. 8. Chromatograms of the flash pyrolysates from perhydrous coals (see Table 6 for peak identification).

Table 6. Compounds identified from flash pyrolysis/gas chromatography/mass spectrometry for the perhydrous coals (for peak code see Fig. 8)

Peak code	Compound	Peak code	Compound
1	Toluene	48	C3-naphthalene
2	C1-thiophene	49	C3-naphthalene
3	C2-benzene	50	Dihdropyrene
4	C2-thiophene	51	9H-fluorene
5	Styrene	52	C3-naphthalene
6	C3-benzene	53	C2-biphenyl
7	Phenol	54	C1-dibenzofuran (several isomers)
8	<i>o</i> -Cresol	55	C1-naphthalenol (several isomers)
9	<i>m</i> -, <i>p</i> -Cresol	56	C2-biphenyl
10	C1-benzofuran	57	C1-naphthalenol
11	2,6-dimethylphenol	58	Cadalene
12	2-ethylphenol	59	C2-naphthalenol (several isomers)
13	2,4-dimethylphenol	60	C2-dibenzofuran (several isomers)
14	4-ethylphenol	61	C3-biphenyl
15	Naphthalene	62	C3-biphenyl
16	C3-phenol	63	Phenanthrene
17	C2-benzofuran	64	Anthracene
18	Vinyl phenol	65	C3-dibenzofuran
19	C3-phenol	66	C3-naphthalenol
20	C3-phenol	67	C3-dibenzofuran
21	C3-alkenyl phenol/indanol	68	C3-naphthalenol
22	C4-phenol	69	C3-dibenzofuran
23	2-methylnaphthalene	70	C4-dibenzofuran
24	C3-phenol	71	C3-naphthalenol
25	1-methylnaphthalene	72	C3-dibenzofuran
26	C4-phenol	73	C1-phenanthrene/anthracene
27	C3-phenol	74	C4-dibenzofuran
28	C3-phenol	75	C1-phenanthrene/anthracene
29	C4-phenol	76	C4-dibenzofuran
30	C3-alkenyl phenol/indanol	77	C1-phenanthrene/anthracene
31	C5-phenol	78	C4-dibenzofuran
32	Biphenyl	79	C4-dibenzofuran
33	C5-phenol	80	C1-phenanthrene/anthracene
34	C4-alkenyl phenol/indanol	81	C4-dibenzofuran
35	C2-naphthalene	82	C4-dibenzofuran
36	C2-naphthalene	83	Fatty acid-C16
37	C4-alkenyl phenol	84	7-hydroxy-cadalene
38	C2-naphthalene	85	C4-naphthalenol
39	C2-naphthalene	86	C4-dibenzofuran
40	Methyl, isopropylbenzene	87	C4-dibenzofuran
41	C1-biphenyl	88	C5-dibenzofuran
42	C1-biphenyl	89	Fatty acid-C18
43	Dibenzofuran	90	2,3-dihydro-2-methyl-4-phenylbenzofuran
44	C3-naphthalene	91	Benzofluorene
45	C3-naphthalene	92	Benzofluorene
46	C3-naphthalene	93	Benzofluorene
47	Naphthalenol		

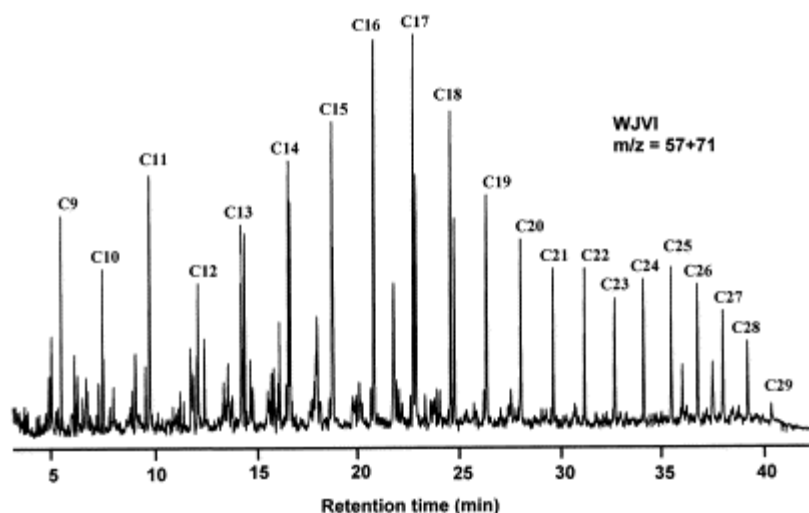


Fig. 9. *n*-Alkanes detected in the pyrolysate of WJVI coal (m/z 57+71 fragmentogram).

For all samples, the highest peaks in the chromatogram are 9 and 13 (Fig. 8). The major contributor to peak 13 is 2,4-dimethylphenol (Table 6). The formation of this compound is believed to occur in the transformation of catechol-like structures into phenolic structures which takes place, in a selective manner, during the coalification process from lignite to the subbituminous coal rank [30 and 33]. Peak 9 is due to the contribution of the *m*- and *p*-cresol isomers (Table 6) which are not separated in the chromatographic conditions used in this work. However, the infrared data which show a great contribution of *para*-substituted aromatic units in the raw coals, suggest that the major contributor to peak 9 is *p*-cresol. This is supported by the correlation between the intensity of peak 9 and the relative intensity of the 815 cm^{-1} mode in the infrared spectra of the samples (%815, Table 3) shown in Fig. 10.

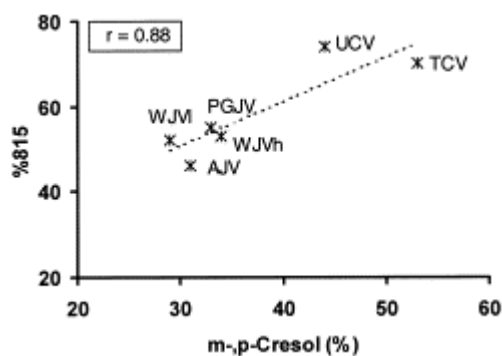


Fig. 10. Relationship between the intensity of peak 9 (*m,p*-cresol) in the chromatograms of the pyrolysates and the relative intensity of the infrared mode at 815 cm^{-1} in the perhydrous coals.

Oxygenated compounds constitute between 79 and 84% of the pyrolysates derived from perhydrous coals (Fig. 11a). The phenol derivatives preponderate (47–56%). Alkenyl phenols/indanols and benzofurans are derived from phenols through secondary reactions [61]. Fig. 11b shows a good linear correlation between the proportion of oxygenated compounds (excluding the products from secondary reactions) in the pyrolysates and the O/C atomic ratio of the raw perhydrous coals.

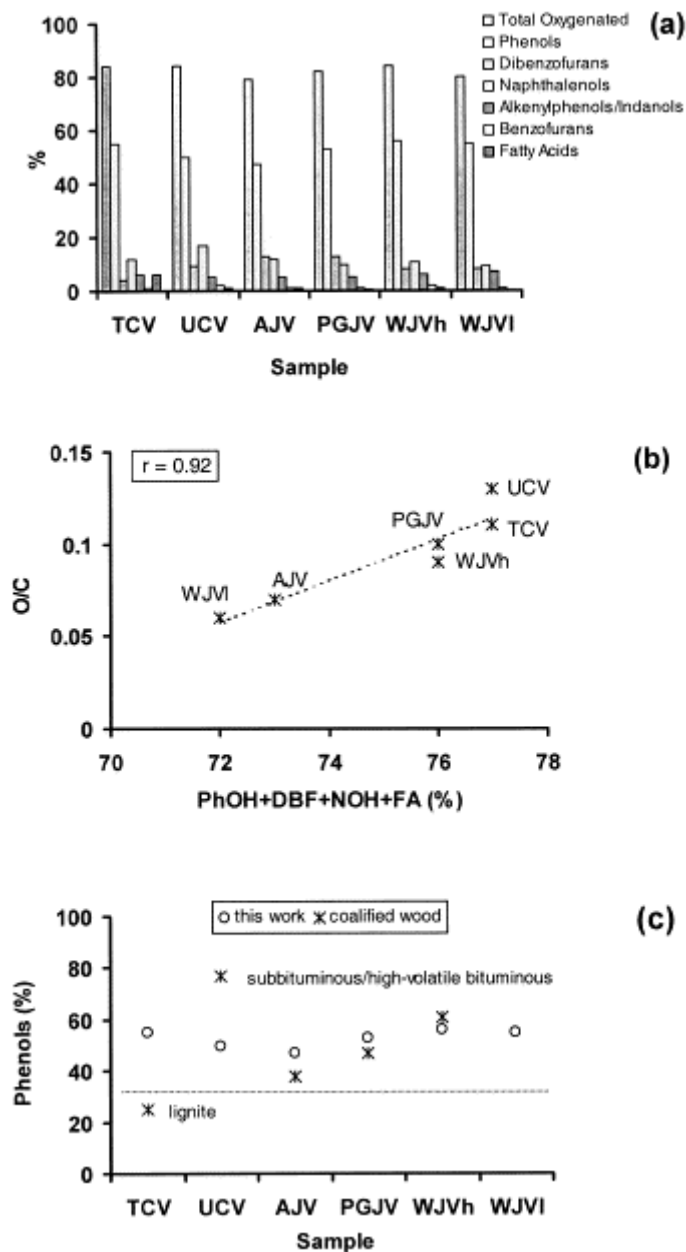


Fig. 11. (a) Concentration of oxygenated compounds in the pyrolysates from perhydrous coals. (b) Correlation between the amount of oxygenated compounds in the pyrolysates and the O/C atomic ratio of the raw coals (oxygenated compounds formed through secondary reactions, *n*-alkenyl phenols/indanols and benzofurans were excluded). (c) Comparison between the concentration of phenol derivatives in the pyrolysates of the perhydrous coals and that reported for pyrolysates from coalified wood of increasing rank [32 and 33].

Chemical structural models for lignin-derived vitrinite [30, 31, 32 and 33] have shown that in the stage of the lignite coal rank there is a preponderance of methoxy-phenol and catechol derivatives and a minor amount of phenol derivatives. With the increase in rank the amount of phenol and alkyl phenols increases up to ca 0.6% of vitrinite reflectance [62]. In the pyrolysates from the perhydrous coals neither catechol nor methoxy phenols were detected (Fig. 8 and Table 6), the amount of phenols in these pyrolysates being very close to that found in samples of subbituminous/high-volatile bituminous coal rank (Fig. 11c).

Fig. 12a shows the contribution of phenol and alkyl phenols to the total amount of phenol derivatives in the pyrolysates. In all cases, phenol and the alkyl phenols from C1 to C3

dominate. TCV and UCV pyrolysates are characterised by a higher amount of phenol and cresol than the other pyrolysates (AJV, PGJV, WJVh and WJVI). According to data in the literature [32], the increase in the degree of substitution of phenol derivatives in the pyrolysates might be related to the increase in rank from subbituminous to high-volatile bituminous. Thus, the values of the phenol and cresol to C2–C4-alkyl phenol ratio and that between *p*-cresol and 2,4-dimethylphenol, higher in the TCV and UCV pyrolysates than in the others (Fig. 12b and c), indicate a lower degree of evolution for these perhydrous coals.

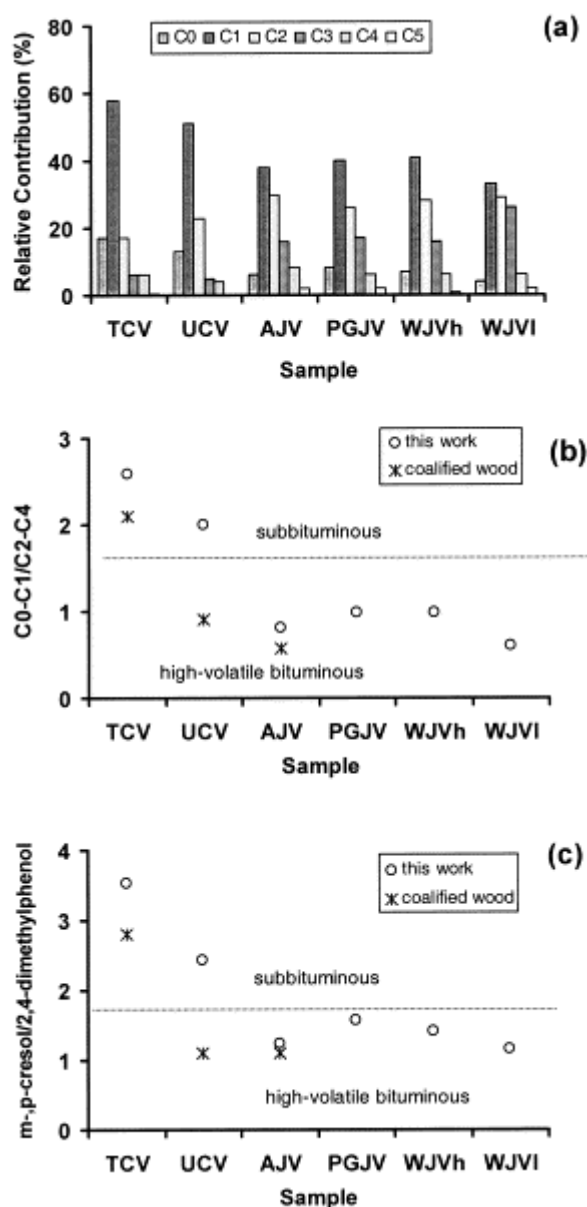


Fig. 12. (a) Contribution of phenol and alkyl phenol derivatives to the total amount of phenols in the pyrolysates. (b) Estimation of the degree of substitution of phenol derivatives (phenol and cresols to C2–C4 alkyl phenols ratio) in the pyrolysates of perhydrous coals and comparison with literature data [33]. (c) Ratio between the intensities of the major phenol isomers (2,4-dimethylphenol and *p*-cresol) from the pyrolysates of perhydrous coals and comparison with literature data [33].

The results obtained agree with the ligneous nature of the perhydrous huminites/vitrinites studied here. They also suggest that lignin in gymnospermous wood is their precursor. However, the results obtained by means of FTIR (clear absorption at 1500 cm^{-1}) and those

related to the composition of the pyrolysates for the perhydrous coals clearly show that the structural reorganisation of the aromatic lignin framework is retarded in these samples, particularly in TCV and UCV, with respect to the evolution of the oxygenated functionalities of the lignin. The increase in vitrinite reflectance has been associated with the structural reorganisation of the aromatic lignin framework [49]. Such reorganisation occurs parallel to the reactions involving oxygenated groups and the concomitant growth of polycyclical aromatic units has been related to the increasing intensity ratio of the aromatic stretching vibration at 1600 and 1500 cm^{-1} in the infrared spectra [49].

Furthermore, the differences found between the TCV, UCV and WJVI pyrolysates derived from samples with very close reflectance values (Table 1) reflect the influence of the hydrogen and/or the source of the high hydrogen content on the evolution process. This influence is also found when the composition of TCV and UCV pyrolysates is compared with that reported for other perhydrous ulminites (huminites) [20] of similar origin and characteristics as TCV and UCV huminites. The ulminites A studied by Syskes et al. [20] have a lower degree of perhydrous character and in the corresponding pyrolysates methoxy phenols preponderate whereas in the TCV and UCV pyrolysates, these compounds are absent.

The contribution of aromatic hydrocarbons in the pyrolysates (Fig. 13a) is low. The AJV, WJVI and PGJV pyrolysates show higher amounts of aromatic hydrocarbons compared to the others, the lowest value corresponding to the TCV pyrolysate. However, according to the real degree of evolution of AJV coal [16] a much higher contribution of alkylbenzenes in the pyrolysate might be expected [32]. Furthermore, taking into account the composition of the volatile fraction of the extracts (Fig. 5), it is likely that hydrocarbons in the pyrolysates derived from the assimilate substances (AJV, PGJV, WJVh and WJVI coals) and from the resinite (TCV and UCV samples) rather than from the coal matrix. In both extracts and pyrolysates derived from the Jurassic samples (AJV, PGJV, WJVh and WJVI) naphthalene derivatives preponderate. Similarly, cadalene was only identified in significant amounts in the TCV and UCV pyrolysates, the amount of this compound being higher in TCV than in the UCV pyrolysate (Fig. 13a). This result agrees with the presence and relative amount of resinite in the raw samples (Table 1). Fig. 13b shows the good linear correlation between the contribution of the condensed aromatic hydrocarbons (naphthalenes, phenanthrenes and benzofluorenes) to the total amount of aromatic hydrocarbons found in the pyrolysates and the relative intensity of the aromatic mode at 870 cm^{-1} (isolated aromatic CH groups, see %870 in Table 3). This result shows the influence that the secondary substances incorporated into the coal matrix of the samples has on the amount of aromatic hydrogen and its distribution.

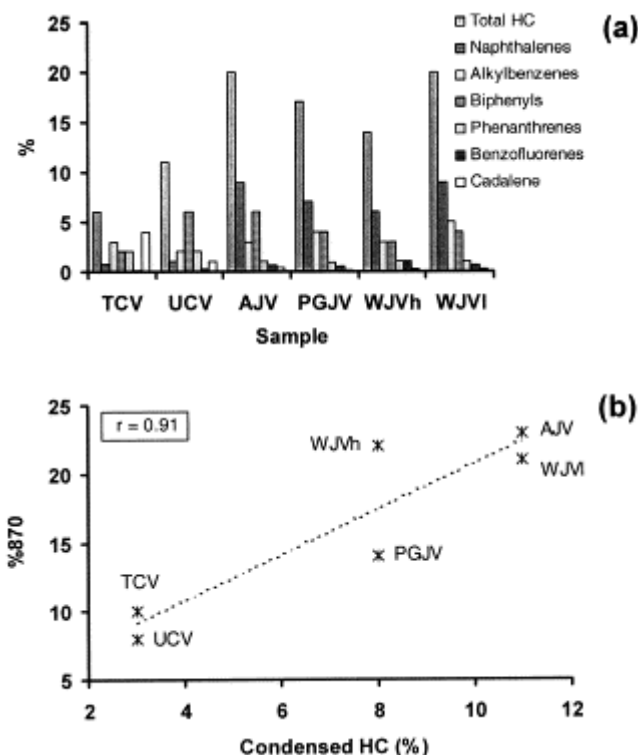


Fig. 13. (a) Concentration of aromatic hydrocarbons in the pyrolysates from perhydrous coals. (b) Relationship between the contribution of condensed aromatic hydrocarbons in the pyrolysates and the relative intensity of the infrared mode at 870 cm⁻¹ in the FTIR spectra of the raw coals.

The difference in the amount of hydrocarbons and their origin in the pyrolysates supports the hypothesis proposed concerning the nature of the perhydrous character of the raw materials. In UCV and particularly in the TCV pyrolysates, the small amount of hydrocarbons indicates that the perhydrous character and peculiar properties of these samples cannot be associated with the incorporation of lipoidal material within the byopolymers derived from lignin, cellulose or tannin. They are rather due to a modification of the botanical precursors, probably in both coals, as a result of the resinization process undergone by the original vegetal tissues. For the UCV coal this hypothesis is supported by the close similarity in the data discussed in this work and, in particular, the close resemblance between the composition of the pyrolysate of this sample and that of TCV. Resinization, typical of conifer woods [17 and 18], also agrees with the botanical origin of Utah jet (family of the Taxodiaceae) proposed by Traverse and Kolvoord [36]. As a result of such modifications, the evolution of the precursor follows a different pathway to the one reported during normal coalification.

In the case of Jurassic coals the results confirm the view that all of the samples contain in their coal matrix secondary substances, derived from the postsedimentary transformations of other different organic materials, which were later incorporated into their structure. Data in Fig. 13a also suggest that the highest (lowest) amounts of these secondary organic substances must be present in the AJV and WJVI (WJVh) samples. The qualitative intensity of fluorescence observed in Jurassic samples seems to agree with the amount and type of aromatic hydrocarbons found in their pyrolysates. This result confirms the view that the fluorescence properties of the huminites in these samples are due to the assimilated substances. Artificial maturation studies [63 and 64] with special emphasis on the presence of hydrocarbons and polar compounds, have shown the important role of the reacting medium for obtaining accurate information about the coalification process. It is clear that the

incorporation of this type of compound during the earlier diagenetic stages of organic evolution must have affected the coalification process. Furthermore, the effect of the subsequent evolution of a vegetal precursor modified by the presence of terpene type resinite or the presence of hydrocarbons (mainly naphthalene and phenanthrene derivatives and also normal alkanes) is expected to be clearly different. Thus the differences found between samples with very close values of vitrinite reflectance (TCV, UCV and WJVI) can be more easily explained.

Finally, in the pyrolysates derived from perhydrous coals organo-sulphur compounds were detected (Fig. 8 and Table 6), but in a very low proportion. This agrees with the low amount of organic sulphur found in the elemental composition of the samples (Table 2). Fig. 14 shows the good linear correlation between the organic sulphur of the elemental analysis and the amount of thiophene derivatives in the pyrolysates.

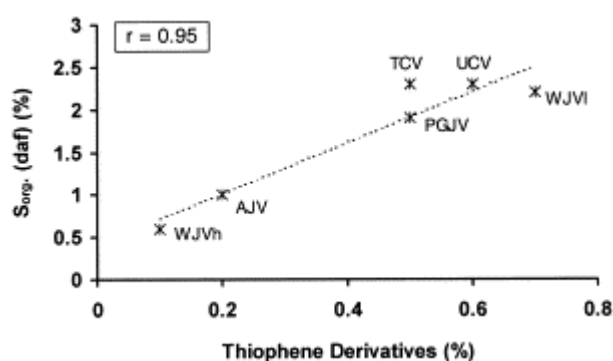


Fig. 14. Relationship between the concentration of the organo-sulphur compounds in the pyrolysates and the amount of organic sulphur (elemental analysis) of the raw coals.

4. Summary

The coals selected for this work are characterised by a perhydrous character of different origin. Besides the high H/C atomic ratio, the coals show a high volatile matter and carbon content, as well as abnormally low values of vitrinite reflectance. They contain aromatic structures with 1–2 rings, mainly *para*-substituted, with a very small contribution of aromatic rings of large size. The results of the FTIR and Py-GC/MS study show that the major structural units in these coals are simple phenols with a preponderance of *para*-alkyl substituted derivatives. Their pyrolysates exhibit the highly phenolic signature typical of lignin-derived material and the distribution of alkyl phenol derivatives suggests a similar pathway to that reported during normal coalification for the alteration of the oxygenated functionalities in the lignin precursor to the phenolic structures of subbituminous coal rank. Nevertheless, during the natural evolution of the perhydrous coals such transformations took place without the parallel structural reorganisation of the aromatic lignin framework responsible for the formation of polycyclical aromatic systems. Consequently, the values of vitrinite reflectance do not increase as might be expected in the diagenetic evolution of normal vitrinites. In addition to these general features, which are common for all of the perhydrous samples studied, clear chemical–structural differences between the huminites/vitrinites were found. These differences are mainly due to the source of the hydrogen content and the effect that it has during the subsequent evolution process of the coals. In spite of the different geological backgrounds of the coals, the results obtained make it possible to divide them in two groups: Cretaceous and Jurassic.

4.1. Cretaceous coals (TCV and UCV): perhydrous character due to the nature of the botanical precursors

The petrographical and geochemical data for these coals show a close similarity. The presence of exsudatinite, and the relatively similar optical properties for both coals suggest they have a similar degree of maturity. Like TCV, the UCV sample represents the beginning of the bituminisation interval but both coals have suppressed reflectance. The Cretaceous samples show a lower (higher) carbon content (O/C atomic ratio) when compared with the same parameters in the case of Jurassic coals. The aromaticity of the Cretaceous samples is also lower than that obtained for the Jurassic coals. Furthermore, in these samples a higher preponderance of *para*-alkyl substituted phenols is typical whereas the degree of substitution of the phenol derivatives in the pyrolysates is lower than in the other samples. All of these results agree with the low degree of evolution of the Cretaceous coals.

Concerning the composition of the pyrolysates, the incorporation of lipoidal material into the biopolymers derived from lignin, cellulose or tannin is discarded as the factor responsible for their perhydrous character and peculiar properties. It is rather due to a modification of the botanical precursors probably in both cases as a result of the saturation of the original vegetal tissues by resin (resinization of tissues). In agreement with this, the volatile fraction of the extracts is made up of the degradation products from terpene-type resinite. Slightly semi-quantitative differences detected in the composition of the soluble organic fractions are probably related to differences in the botanical precursors of these coals and to the physico-chemical conditions that existed in the corresponding depositional environment. The modification of the vegetal tissues by the presence of terpene-type resinite affected the evolution of the samples. It inhibits a normal increase in huminite reflectance and favours its suppression.

4.2. Jurassic coals (AJV, PGJV, WJVh and WJVI): perhydrous character related with the assimilation of highly hydrogenated secondary products

The characteristics and properties described for the Jurassic coals clearly show that they all contain secondary substances from the postsedimentary transformations of other different organic material in their coal matrix. The incorporation of these secondary compounds (mainly naphthalene and phenanthrene derivatives and also normal alkanes in the case of WJVh and particularly in WJVI coals) modifies the reacting medium in which the process of natural coalification takes place. This explains why the evolution pathway followed by these coals is different to that usually described for the natural coalification of non-perhydrous coals with an anomalous increase in vitrinite reflectance. The effect that the incorporation of the aromatic hydrocarbons has on the organic evolution must be different to that which occurred in the case of perhydrous coals produced by the modification of the botanical precursor. This is due to the different source that supplies the hydrogen, but especially to the different level of organic evolution in which the process of hydrogen-enrichment occurs, as is clearly shown in the differences found between the WJVI and WJVh, and TCV and UCV coals.

The extent of impregnation by secondary substances of Jurassic coals is not the same and differences in the nature of the assimilated compounds are also found, affecting not only the aliphatic material but also the aromatic compounds and the interactions between them and the coal matrices.

Acknowledgements

Financial support for this work was provided through a contract with the European Community (No. 7220/EC-769). The authors thank Dr A. Jiménez (from the University of Oviedo, Spain) and Mr J. R. Montes (from INCAR — CSIC, Spain) for some experimental analyses and the preparation of some samples. Finally, the authors thank the two anonymous referees for their constructive comments.

References

1. J. Newman and N.A. Newman *N.Z.J. Geol. Geophys.* **25** (1982), p. 233.
2. M. Teichmüller, In: Coal and Coal Bearing Strata: Recent Advances. Geol. Soc. Spec. Publ. vol. 32 (1987) p. 127.
3. W.J.J. Fermont *Org. Geochem.* **12** (1988), p. 401.
4. M.G. Fowler, T. Gentzis, F. Goodarzi and A.E. Foscolos *Org. Geochem.* **17** (1991), p. 805.
5. H. Fang and C. Jianyu *J. Petrol. Geol.* **15** (1992), p. 419.
6. J.C. Quick In: P.K. Mukhopadhyay and W.G. Dow, Editors, *Vitrinite Reflectance as a Maturity Parameter. Applications and Limitations* ACS Symp. Ser. **570**, American Chemical Society, Washington, DC (1994), p. 64.
7. B.A. Stankiewicz, M.A. Kruge and M. Mastalerz *Org. Geochem.* **24** (1996), p. 531.
8. H.I. Petersen and P. Rosenberg *J. Petrol. Geol.* **21** (1998), p. 247.
9. L.W. Gurba and C.R. Ward *Int. J. Coal Geol.* **36** (1998), p. 111.
10. A.C. Hutton and A.C. Cook *Fuel* **59** (1980), p. 711.
11. M. Teichmüller *Int. J. Coal Geol.* **20** (1992), p. 1.
12. S. Watts, A.M. Pollard and G.A. Wolff *Archeometry* **39** (1997), p. 125.
13. M. Mastalerz, K.R. Wilks and R.M. Bustin *Org. Geochem.* **20** (1993), p. 555.
14. T. Gentzis and F. Goodarzi In: P.K. Mukhopadhyay and W.G. Dow, Editors, *Vitrinite Reflectance as a Maturity Parameter. Applications and Limitations* ACS Symp. Ser. **570**, American Chemical Society, Washington, DC (1994), p. 93.
15. H.I. Petersen and H. Vosgerau *Int. J. Coal Geol.* **41** (1999), p. 257.
16. I. Suárez-Ruiz, M.J. Iglesias, A. Jiménez, F. Laggoun-Défarge and J.G. Prado In: P.K. Mukhopadhyay and W.G. Dow, Editors, *Vitrinite Reflectance as a Maturity Parameter.*

Applications and Limitations ACS Symp. Ser. **570**, American Chemical Society, Washington, DC (1994), p. 76.

17. E. Stach, M.Th. Mackowsky, M. Teichmüller, G.H. Taylor, D. Chandra and R. Teichmüller In: *Textbook of Coal Petrology* (3rd ed.), Gebruder Borntraeger, Berlin (1982).

18. G.H. Taylor, M. Teichmüller, A. Davis, C.F.K. Diessel, R. Littke and P. Robert *Organic Petrology. A new handbook incorporating some revised parts of Stach's Textbook of Coal petrology* (1st ed.), Gebruder Borntraeger, Berlin (1998).

19. F.T.C. Ting and J-A. Sitler *Org. Geochem.* **14** (1989), p. 247.

20. R. Syskes, M.G. Fowler and K.C. Pratt *Energy & Fuels* **8** (1994), p. 1402.

21. E. Zhang, P.G. Hatcher and A. Davis *Org. Geochem.* **20** (1993), p. 721.

22. S.A. Stout and J.J. Boon *Org. Geochem.* **21** (1994), p. 953.

23. I. Suárez-Ruiz, A. Jiménez, M.J. Iglesias, F. Laggoun-Défarge and J.G. Prado *Energy & Fuels* **8** (1994), p. 1417.

24. L.C. Price and C.E. Barker *J. Petrol. Geol.* **8** (1985), p. 59.

25. A. Jiménez, M.J. Iglesias, F. Laggoun-Défarge and I. Suárez-Ruiz *Chem. Geol.* **150** (1998), p. 197.

26. Z.S. Smutkina, V.I. Sekrieru, T.A. Titova and G.B. Skripchenko *Solid Fuel Chemistry* **16** (1982), p. 53.

27. S. Creaney, D.E. Pearson and L.G. Marconi *Fuel* **59** (1980), p. 438.

28. B.-P. Perrusel, F. Laggoun-Défarge, I. Suárez-Ruiz, A. Jiménez, M.J. Iglesias and J.-N. Rouzaud In: B.Q. Li and Z.Y. Liu, Editors, *Prospects for Coal Science in the 21st Century*, Sanxi Science & Technology Press, Taiyuan, P.R. China (1999), p. 145.

29. M.J. Iglesias, A. Jiménez, F. Laggoun-Défarge and I. Suárez-Ruiz *Energy & Fuels* **9** (1995), p. 458.

30. P.G. Hatcher, H.E. III Lerch and T.V. Verheyen *Int. J. Coal Geol.* **13** (1989), p. 65.

31. P.G. Hatcher *Org. Geochem.* **16** (1990), p. 959.

32. P.G. Hatcher, J.-L. Faulon, K.A. Wenzel and G.D. Cody *Energy & Fuels* **6** (1992), p. 813.

33. P.G. Hatcher, H.E. Lerche, III, R. Kotra and T.V. Verheyen *Fuel* **67** (1988), p. 1069.

34. C.E. Burgess and H.H. Schobert *Energy & Fuels* **12** (1998), p. 1212.

35. X. Querol, J.L. Fernandez, J.W. Hagemman, J. Dehmer, R. Juan and C. Ruiz *Int. J. Coal Geol.* **18** (1991), p. 327.

36. A. Traverse and R.W. Kolvoord *Science* **159** (1968), p. 302.
37. M. Valenzuela, J.C. García-Ramos, C. Suárez de Centi, *Trabajos de Geología* 16 (1986) 121. University of Oviedo, Spain.
38. I. Suárez-Ruiz and J.G. Prado In: C. Snape, Editor, *Composition, Geochemistry and Conversion of Oil Shales NATO ASI series, Series C: Mathematical and Physical Sciences* **455** (1995), pp. 387–394.
39. H. Muller, in: *Jet*, (1987) Butterworths and Co. Ltd.
40. C. Teixeira, G. Zebyszewski, C. Torre de Assunção, G. Manuela "Carta Geologica de Portugal" Noticia Explicativa da Folha 23-C: Leira. Na Escala 1/50.000. Serviços Geológicos de Portugal. Direcção Geral de Minas e Serviços Geológicos. Ministerio da Economia. Lisboa, (1968).
41. F.F. Helmdach, "Stratigraphy and Ostracod-Fauna from the Coalmine Guimarota (Upper Jurassic)". In: *Contribuição para o conhecimento da fauna do Kimeridgiano da Mina de Lignito Guimarota (Leira, Portugal). II parte. Memoria 17*, (1971) 42-88, Serviços Geológicos de Portugal. Direcção Geral de Minas e Serviços Geológicos. Ministerio da Economia. Lisboa.
42. J. Espitalie, G. Deroo, F. Marquis, *Rev. Inst. Fr. Petrol.* 40/5 (1985) 563, 40/6 755.
43. J. Espitalie, G. Deroo and F. Marquis *Rev. Inst. Fr. Petrol.* **784 4171** (1986), p. 73.
44. A. Jiménez, M.J. Iglesias, F. Laggoun-Défarge and I. Suárez-Ruiz *J. Anal. App. Pyrolysis* **50** (1999), p. 117.
45. A.M. Pollard, G.D. Buseel and D.C. Baird *Archeometry* **23** (1981), p. 139.
46. D.W. van Krevelen *Coal*, Elsevier (1961).
47. M. Teichmüller and B. Durand *Int. J. Coal Geol.* **2** (1983), p. 197.
48. M. Radke, H. Willsch and M. Teichmüller *Org. Geochem.* **15** (1990), p. 539.
49. H.J. Schenk, E.G. Witte, R. Littke and K. Scwochau *Org. Geochem.* **16** (1990), p. 943.
50. R.M. Eloffson *J. Can. Chem.* **35** (1957), p. 926.
51. J.V. Ibarra, E. Muñoz and R. Moliner *Org. Geochem.* **24** (1996), p. 725.
52. L.J. Bellamy In: *The Infrared Spectra of Complex Molecules I*, Chapman and Hall (1975), p. 72.
53. M.J. Iglesias, A. Jiménez, J.C. del Río, I. Suárez-Ruiz, *Org. Geochem.*, 31 (12) (2000) p. 1285.
54. J.K. Brown, *J. Chem. Soc., London* (1955) 744.

55. E.J. Gallegos *Anal. Chem.* **45** (1973), p. 1399.
56. C.M. White and M.L. Lee *Geochim. Cosmochim. Acta* **44** (1980), p. 1825.
57. R. Dutta and H.H. Schobert In: K.B. Anderson and J.C. Crelling, Editors, *Amber, Resinite and Fossil Resins ACS Symp. Ser.* **617**, American Chemical Society, Washington, DC (1995), p. 263.
58. H. Solli, S.R. Larter and A.G. Douglas *J. Anal. Appl. Pyrolysis* **1** (1980), p. 231.
59. M. Radke, H. Willsch, D. Leythaeuser and M. Teichmüller *Geochim. Cosmochim. Acta* **46** (1982), p. 1831.
60. R. Alexander, R.I. Kagi, S.J. Rowland, P.N. Sheppard and T.V. Chirila *Geochim. Cosmochim. Acta* **49** (1985), p. 385.
61. J.V. Christiansen, A. Feldthus and L. Carlsen *J. Anal. Appl. Pyrolysis* **32** (1995), p. 51.
62. M.I. Venkatesan, K. Ohta, S.A. Stout, S. Steinberg and J.L. Oudin *Org. Geochem.* **20** (1993), p. 463.
63. L. Mansuy, P. Landais and O. Ruau *Energy & Fuels* **9** (1995), p. 691.
64. L. Mansuy and P. Landais *Energy & Fuels* **9** (1995), p. 809.